# ADP-Ribosyltransferase PARP11 Suppresses Zika Virus in Synergy with PARP12

**Lili Li**
Suzhou institute of systems medicine
**Yueyue Shi**
Suzhou institute of systems medicine
**Sirui Li**
University of North Carolina at Chapel Hill
**Junxiao Liu**
Suzhou institute of systems medicine
**Shulong Zu**
Institute of Basic Medical Sciences
**Xin Xu**
Suzhou institute of systems medicine
**Meiling Gao**
Suzhou institute of systems medicine
**Nina Sun**
Institute of Basic Medical Sciences
**Chaohu Pan**
Suzhou institute of systems medicine
**Linan Peng**
Suzhou institute of systems medicine
**Heng Yang** ( yhmyt@hotmail.com )
Suzhou institute of systems medicine https://orcid.org/0000-0002-6713-2783
**Genhong Cheng**
University of California Los Angeles

**Research**

**Keywords:** ADP-ribosyltransferase, PARP11, PARP12, Zika virus, NS1 and NS3, anti-viral ISGs

**Posted Date:** April 7th, 2021

**DOI:** https://doi.org/10.21203/rs.3.rs-385154/v1

# Abstract

Zika virus (ZIKV) infection and ZIKV epidemic have been continuously spreading silently throughout the world and its associated microcephaly and other serious congenital neurological complications poses a significant global threat to public health. ZIKV infection stimulates type I interferon response in host cells which suppresses viral replication by inducing the expression of interferon-stimulated genes (ISGs). Here, we identified ADP-ribosyltransferase *PARP11* as an anti-ZIKV ISG and found that PARP11 suppressed ZIKV independently on itself PARP enzyme activity. Furthermore, PARP11 interacted with PARP12 and promoted PARP12-mediating ZIKV NS1 and NS3 protein degradation. Homo family PARP11 and PARP12 cooperated with each other on ZIKV suppression and the anti-ZIKV function of PARP11 mostly dependent on the existence of PARP12. Our findings have broadened the understanding of the anti-viral function of PARP11, and more importantly suggest a potential therapeutics target against ZIKV infection.


# Introduction

Zika virus (ZIKV) was first isolated in 1947 in the Zika forest of Uganda from an infected rhesus macaque (1). Since its discovery, ZIKV stayed relatively silent for almost 70 years and all of a sudden all over the America after Pacific Islands to Brazil. By December 2015, 18 states of Brazil had reported autochthonous ZIKV transmission and large numbers of cases of microcephaly and infection were reported in 2015 and 2016 (2–4). On February 1, 2016, the World Health Organization (WHO) declared ZIKV outbreak and its associated clinical manifestations as a Public Health Emergency of International Concern (PHEIC). ZIKV continues to develop and spread silently throughout the world in the form of asymptomatic infections. During September-November 2018, the biggest Indian break was reported from Rajasthan and Madhya Pradesh states of India. Up to July 2019, 87 countries reported ZIKV transmission and 1274974 diagnosed cases were reported in Brazil (5). Recently, a research found Africa strain ZIKV infection in Brazil (the prevalent strain was Asia strain) and suggested more attention should be paid to another outbreak of ZIKV epidemic (6).

ZIKV infection is asymptomatic in up to 80% adults, the remaining 20% infected adults are characterized by low fever, arthralgia, maculopapular rash accompanied by pruritis, and conjunctivitis. Moreover, ZIKV infection in adults was associated with Guillain-Barre syndrome and infection during pregnancy can cause infants' microcephaly, intrauterine growth restriction and other birth defects (7–9). Thousands of increased cases of fetal abnormalities, including microcephaly, were reported up to February 2016 in ZIKV infected areas (9–11). At present, vaccines or antivirals to treat ZIKV infection are unavailable (12–14). Thereby, a comprehensive research for anti-ZIKV genes and more potential therapy targets are urgently needed to be identified.

Type I interferon (IFN I) and interferon stimulated genes (ISGs) constitute the vital part of innate immune system against virus infection in vertebrate. Viral infection induces the production of IFN and about 300 ISGs which exert a broad-spectrum anti-viral effect. The potential of IFN and ISGs against ZIKV infection has been indicated (15–17). Our previously work also identified *CH25H* and *PARP12* as critical anti-ZIKV

ISGs who restricted the replication of ZIKV and provided potential therapeutics application (18, 19). Still, many ISGs involved in ZIKV replication are not yet elucidated. The family of poly-adenosine 5'-diphosphate (ADP)-ribose polymerases (PARPs), also known as ADP-ribosyltransferases, which mediate a unique translational modification called ADP-ribosylation by transferring of ADP-ribose from nicotinamide adenine dinucleotide ($NAD^+$) to target proteins (20–22). Among the 17 PARPs expressed in human cells, several PARPs, such as PARP13, PARP9, PARP10, PARP14, PARP12 and PARP5, have been identified as ISGs and are involved in anti-viral response (23–25). In an anti-ZIKV ISGs screening work we reported mono ADP-ribosyltransferase PARP11 with anti-ZIKV function but without detailed mechanism described (18). Lastly, Guo *et al* reported that PARP11 promotes vesicular stomatitis virus (VSV) and herpes simplex virus-1 (HSV-1) infection by inhibiting the interferon antiviral response (26). These results indicate a complex involvement of PARP11 in different viral infection.

In this work, we found that PARP11 is up-regulated in response to IFN I signaling pathway and ZIKV infection, and PARP11 was proved to suppress the replication of ZIKV. Unlike that PARP12 suppresses ZIKV by degrading NS1 and NS3 proteins dependent on its PARP enzyme activity, PARP11 suppresses ZIKV independent on itself PARP enzyme activity but by the cooperation with PARP12. These findings that PARP11 interacts and cooperates with PARP12 in ZIKV suppression could contribute to the treatment of ZIKV infection, and provide a new sight on understanding the role of PARP11 in viral infection.

# Results

### Type I IFN induced PARP11 suppresses ZIKV replication.

In our previously screening for ISGs with activity against ZIKV, we have identified PARP12 that suppresses ZIKV through PARP-dependent degradation of NS1 and NS3 viral proteins (18). We also noticed that the homo-family protein PARP11 showed anti-ZIKV activity. PARP11 was reported as an ISG. To characterize the induction of PARP11 by IFN, we stimulated WT and IFNα/β receptor subunit 1 (IFNAR1)-deficient HEK293T and A549 cells with human IFN I (IFN-α and IFN-β) and quantified the mRNA level of *PARP11* by quantitative real-time PCR (qRT-PCR). We found that increased *PARP11* mRNA was induced by IFN I in WT HEK293T and A549 cells (Fig. 1A and B). The absence of IFN I receptor impaired IFN signaling pathway, so no significant *PARP11* mRNA changed in *IFNAR1*$^{-/-}$ cells (Fig. 1A and B).

Similar to exogenous IFN treatment, ZIKV infection also induced *PARP11* mRNA expression in WT A549 cell but not in *IFNAR1*$^{-/-}$ A549 cells (Fig. 1C). To further identified the anti-ZIKV activity, we generated both *PARP11*-knockout (Figure S1A-C) and PARP11-overexpressing (Figure S1D) A549 cells. We found that ZIKV replication was suppressed in PARP11-overexpressing cells (Fig. 1D and E). Conversely, ZIKV replicated more robustly in *PARP11*-knockout cells (Fig. 1F and G). These results indicate that *PARP11* is an anti-ZIKV ISGs induced by IFN I and ZIKV infection.

### PARP11 suppresses ZIKV independent on the regulation of IFNAR1 protein level

A recently report indicates that PARP11 inhibits the interferon antiviral response by mono ADP-ribosylating the ubiquitin E3 ligase β-TrCP and regulating the protein level of IFNAR1 (26). In this study, Guo *et al* found that PARP11 promotes the replication of VSV and HSV-1 by mediating IFNAR1 ubiquitination and degradation to restrict IFN I induced antiviral efficacy.

In our screening and validation results, however, we proved that PARP11 suppressed ZIKA replication (Fig. 1D-G). The antiviral role of PARP11 observed in ZIKA was different from the conclusion reported by Guo *et al.* To test whether PARP11 suppressed ZIKA by regulating protein level of IFNAR1, we infected WT A549 cells with VSV and ZIKV and detected protein level of IFNAR1 by Western blotting. The result showed that ZIKV infection did not obviously change IFNAR1 protein level, while VSV infection decreased IFNAR1 protein level significantly (Fig. 2A). Then, WT and *PARP11*$^{-/-}$ A549 cells were infected with VSV and ZIKV and protein levels of IFNAR1 were analyzed. In WT A549 cells, VSV infection but not ZIKV infection decreased IFNAR1 protein level. However, IFNAR1 protein level showed no obviously change in both VSV and ZIKV infected *PARP11*$^{-/-}$ A549 cells (Fig. 2B). These results suggest that PARP11 suppressed ZIKV independent on regulation of IFNAR1 protein level. Furthermore, we compared ISGs expression in ZIKV and VSV infected A549 cells and found that both ZIKV and VSV infection stimulated IFN signaling pathway and induced the expression of ISGs (Fig. 2C), suggesting that no obviously defection and difference in IFN signaling pathway and ISGs induction upon ZIKV and VSV infection. As an ADP-ribosyltransferase, whether PARP11 suppressed ZIKV by regulating the ADP-ribosylation of host cells? To test this, we detected ADP-ribosylation of proteins from WT and *PARP11*$^{-/-}$ cells infected by ZIKV and mock control. When PARP11 was knocked out, ADP-ribosylation in host cells was prominently decreased (Fig. 2D). These results indicate that PARP11 suppresses ZIKV independent on the regulation of IFNAR1, and PARP11 impacts ADP-ribosylation level of ZIKV infected host cells.

**PARP11 suppresses ZIKV independent on itself PARP enzyme activity.**

PARP11 contains WWE domain at the N terminus and PARP domain at the C terminus. The WWE domain is a common interaction module that participates in both ubiquitination and ADP-ribosylation (27). The PARP domain is where the PARP enzyme activity located that mediates the posttranslational modification of target proteins (28, 29). The $Gly^{205}$ within the PARP domain of human PARP11 binds the amide group of $NAD^+$, which is essential for PARP enzyme activity. To identify whether PARP11 regulated ADP-ribosylation of ZIKV infected host cells dependent on its PARP enzyme activity, we constructed PARP11 PARP domain deletion mutants and enzyme activity lost mutant (PARP11 G205A) (Fig. 3A). The expression and expected protein size of the mutants were verified by Western blotting (Fig. 3B). Then the mutants were transfected into HeLa cells that were subsequently infected by ZIKV to determine how the different domain and PARP enzyme activity affected viral infection. Cell expressing full-length PARP11 or enzyme lost PARP11 showed similar rates of ZIKV suppression, whereas cell expressing the WWE domain, PARP domain or PARP domain PARP enzyme activity lost mutants showed no suppression on ZIKV replication (Fig. 3C). These results indicate that PARP11 suppresses ZIKV independent on itself PARP enzyme activity and full-length protein.

## PARP11 promotes ZIKV NS1 and NS3 protein degradation mediated by PARP12.

In our previously work, we identified PARP12 suppressed ZIKV through PARP-dependent degradation of NS1 and NS3 viral protein. The PARP enzyme activity of PARP12 is essential for ZIKV suppression. However, in this work, we found that PARP11 suppressed ZIKV independent on itself PARP enzyme activity but can regulated ADP-ribosylation of ZIKV infected host cells. Whether PARP11 suppressed ZIKV in synergy with PARP12 and impacted on the ADP-ribosylation of infected cells utilizing the PARP enzyme activity of PARP12? To test this speculation, we co-transfected HEK293T cells with His-NS1 and NS3, HA-PARP12, YFP-PARP11 or Flag-PARP13 as control, and protein levels were detected by Western blotting. Compared to PARP12 co-transfected with vector group, PARP12 co-transfected with PARP11 reduced the abundance of NS1 and NS3 protein but not in PARP12 co-transfected with PARP13 group (Fig. 4A). This result suggests that PARP11 accelerates the degradation of NS1 and NS3 proteins in synergy with PARP12. To further confirm this conclusion, we further generated *PARP11*$^{-/-}$ HEK293T cell by CRISPR/Cas9 gene knockout system. When endogenous PARP11 was knocked out, the efficient of PAPR12 on NS1 and NS3 degradation was decreased (Fig. 4B). Also, PARP12 showed frustrated NS1 and NS3 degradation ability in *PARP11*$^{-/-}$ HEK293T cells. When PARP11 was transfected back, NS1 and NS3 degradation mediated by PARP12 was increased (Fig. 4C). Then we examined the PAPR11 mutants on NS1 and NS3 degradation when co-transfected with HA-PARP12. Only the full-length and PARP enzyme lost mutation accelerated NS1 and NS3 degradation in synergy with PARP12, the WWE domain, PARP domain and the PARP domain with PARP enzyme lost mutation did not show impact on NS1 and NS3 degradation (Fig. 4D). Together, these results show that PARP11 promotes the degradation of ZIKV NS1 and NS3 proteins in synergy with PARP12.

## PARP11 suppresses ZIKV mostly dependent on PARP12.

All the results above suggested that PARP11 accelerated NS1 and NS3 degradation mediated by PARP12. PARP12 degraded NS1 and NS3 viral protein partly dependent on the existence of PARP11. To prove whether PARP11 suppressed ZIKV dependent on PARP12, we further overexpressed PARP11 in *PARP12*$^{-/-}$ A549 cells and compared the replication of ZIKV in WT, PARP11-overexpressing, *PARP12*$^{-/-}$ and PARP11-overexpressing *PARP12*$^{-/-}$ A549 cells. The results showed that PARP11-overexpressing can both efficiently inhibit ZIKV replication in WT and *PARP12*$^{-/-}$ A549 cells, while ZIKV replication more robustly in PARP11-overexpressing *PARP12*$^{-/-}$ A549 cells when compared with PARP11-overexpressing WT A549 cells (Fig. 5A-C). This result suggested that PARP12 deficiency vastly impaired the anti-viral ability of PARP11. We then checked whether the degradation of NS1 and NS3 mediated by PARP11 was also impacted by PARP12. Western blot analysis revealed that PARP11 can still degradation NS1 and NS3 in *PARP12*$^{-/-}$HEK293T cells but the efficiency was significantly lower than that in WT HEK293T cells (Fig. 5D). These results suggest that PARP11 suppresses ZIKV mostly dependent on the existence of PARP12.

## PARP11 interacts and co-localizes with PARP12.

To elucidate the mechanism by which PARP11 suppressed ZIKV in cooperation with PARP12, we firstly examined the interaction between PARP11 and PARP12. We demonstrated that PARP11 could interact and co-localized with PARP12 protein by co-immunoprecipitation and immunofluorescence assay (Fig. 6A and B). To further identify the protein module of PARP11 that interacted with PARP12, we co-transfected HEK293T cells with HA-PARP12 and EGFP-PARP11 WWE and PARP domain expressing plasmids and performed co-immunoprecipitation assay with HA-tagged agarose beads. Full-length PARP12 interacted with the WWE domain of PARP11 but not the PARP domain (Fig. 6C). This result is in line with the function of WWE domain that is a common interaction module that participates in both ubiquitination and ADP-ribosylation. These results indicated that homo-family protein PARP11 and PARP12 interacted and cooperated with each other on ZIKV suppression.

# Discussion

ZIKV spreads through the world in 2015–2017 and continues to develop and evolution in a form of asymptomatic infectious. According to a lastly report, researchers firstly detected the appearance of the ZIKV Africa lineage in Brazil, indicating the risk of a new epidemic (6). Research on the pathology of ZIKV to explore for available means on epidemic control and associated disease treatment is still on urgently needed. In our previously work, we identified PARP12 with anti-ZIKV function and the detailed mechanism was provided (18). Here, we found that PARP11 suppresses ZIKV in cooperated with its homo-family protein PARP12. These results describe a novel mechanism of PARP11 in viral restriction that is quite different from the report which found that PARP11 promotes VSV and HSV replication by degrading IFNAR1 and inhibiting IFN signaling pathway (26). We speculate the different function of PARP11 may result from different virus species. Indeed, we observed no significant change of IFANR1 at protein level in ZIKV infected A549 WT and PARP11-deficency cells (Fig. 2A and B), indicating different molecular accidents in various virus infection process. We speculated the different function of PARP11 may be a result from the characteristic of different virus species.

In this work, we identified a new anti-ZIKV ISG *PARP11* that suppresses ZIKV in cooperation with PARP12. Several PAPRs have been found with anti-viral function dependent or independent on their PARP enzyme activities. PARP12, for an example, can utilize its PARP enzyme activity to poly ADP-ribosylate ZIKV NS1 and NS3 proteins which mediates their subsequently ubiquitination and degradation by proteasome (18). PARP13, also known as ZnF antiviral protein (ZAP), inhibits various viruses by directly viral mRNA or protein degrading independent on its PARP enzyme activity (30). PARP11 was reported as a novel enzyme important for proper sperm head shaping and a potential factor involved in idiopathic mammalian teratozoospermia. In this process PARP11 exhibits mono ADP-ribosylation activity which ADP-ribosylates itself and are essential for colocalization of PARP11 with the nuclear pore components (31). Other research also indicated that the cellular location of PARP11 is regulated by its PARP catalytic activity (32). In this work, we found that PARP11 suppresses ZIKV independent on itself PARP enzyme activity but still up-regulates the ADP-ribosylation level of proteins in host cells. We proved that the existence of PARP11 accelerates the degrading of NS1 and NS3 mediated by PARP12. Meanwhile, the anti-viral function of PARP11 was obviously impaired when PARP12 was knocked out, indicating that

PARP11 inhibits ZIKV dependent on the existence of PARP12. These results suggest that PARP11 cooperates with PARP12 in ZIKV protein degradation. The current work and Guo *et al* work shows the vital role of PARP11 in viral defense. However, PARP11 suppresses ZIKV and degrades ZIKV NS1 and NS3 proteins, even at a much low efficiency, in the absence of PARP12. So, other unrevealed mechanism might be involved in a manner of independent on IFNAR1 degradation and cooperation with PARP12. Until now, there is not too much work about the anti-viral function of PARP11. Thus, more attention should be paid to the anti-viral role of PARP family proteins, especially PARP11 and PARP12.

We further identify PARP11 interacts with PARP12 through its WWE domain. Considering that PARP12 ADP-ribosylates NS1 and NS3 dependent on PARP enzyme activity, PARP12 may work as an intermediate that interacts with NS1 and NS3 proteins by its PARP domain and interacts with PARP11 by its WWE domain. PARP11, NS1 and NS3 proteins, and PARP12 constitute a degradation complex in which PARP11 assists PARP12 in an unknown mechanism.

Together, our work highlights a novel anti-ZIKV mechanism of PARP11 and the complicated role of PARP11 in various virus infection, providing more reference on anti-ZIKV treatment.

# Materials And Methods

### Virus and cells

ZIKV strain GZ01/2016 (Genbank accession number KU820898) and VSV virus was used at a multiplicity on infection (MOI) of 0.1 in this study, except where indicated otherwise (33). The *IFNAR1*$^{-/-}$ HEK293T and A549 cell lines were generated as described (19). A549, BHK-21, Vero, HeLa and HEK293T cells were purchased from America Type Culture Collection and cultured in Dulbecco's modified Eagle's medium (DMEM) (37°C, 5% $CO_2$) supplemented with 10% fetal bovine serum (FBS),100U/mL penicillin and 50 μg/mL streptomycin.

### Plaque assay

BHK-21 cells were seeded in a 12-well plate for 12 hr. Cells were washed with PBS once and infected with virus samples for 1 hr. The culture supernatant was aspirated and replaced with DMEM containing 1% low-melting agarose and 2% FBS. Viral plaques were stained and counted 4 days after infection. The titer of ZIKV was quantified by plaque assay and normalized to control.

### DNA constructs and stable cell line generation

pMOI-GFP and pMOI-PARP11 (Homo sapiens) expression plasmids were purchased from GeneCopoeia and described previously (34). The viral RNA of the GZ01/2016 strain was isolated and used in reverse transcription PCR experiments to obtain the complementary DNA (cDNA) sequence of ZIKV nonstructural NS1 and NS3 proteins. ZIKV NS1 and NS3 genes were cloned into the pcDNA6/V5-His expression vector (Invitrogen) using standard molecular techniques and verified by sequencing. DsRed-PARP11, EGFP-

PARP12, Flag-PARP11, HA-PARP12, EGFP-PARP11 WWE domain, EGFP-PARP11 PARP domain, YFP-PARP11, Flag-PARP13 and HA-PARP11 mutants were cloned using standard molecular cloning and oligonucleotide mutagenesis methods. To create a stable cell line for PARP11 expression, PARP11 was cloned into the pMXsIG-lgkFLAG vector and co-transfected into HEK293T cells with VSV glycoprotein and pCpG helper plasmids. 48 hr after transfection, the culture supernatant was collected and added into WT or *PARP12*$^{-/-}$ A549 cells for infection. The cells were collected 72 hr after infection, and the PARP11-overexpressing cells were then sorted by fluorescence-activated cell sorting (FACS).

### Western blotting

WT, *PARP11*$^{-/-}$ and *PARP12*$^{-/-}$ HEK293T cells were cotransfected with the plasmids listed in the main text and where indicated. 28 hr after transfection, cells were treated with lysis buffer [ 50mM tris-HCl (pH 7.5), 150 mM NaCl, 5 mM EDTA, 1% NP-40, 1 mM PMSF, and 1xprotein inhibitor (Roche)]. The cell extracts were immunoblotted with the indicated antibodies to measure the level of the expressed proteins. Mouse anti-β-actin (ZSGB-Bio), rabbit anti-GFP (Abcam), rabbit anti-PARP11 (Thermo Fisher Scientific), mouse anti-poly(ADP-ribose) (GeneTex) and mouse anti-HA, anti-His, and anti-Flag tag antibodies (Sigma-Aldrich) were used for detection at the appreciated dilutions.

### Co-immunoprecipitation assay

HEK293T cells were transfected with the indicated plasmids. 30 hr after transfection, protein was extracted using solution A [ 50mM tris-HCl (pH 7.5), 150 mM NaCl, 5 mM EDTA, 1% Triton-X100, 1 mM phenylmethylsulfonylfluoride (PMSF), and 1xprotein inhibitor (Roche)]. An aliquot of the extracts was immunoblotted with the indicated antibodies. The remaining extracts were immunoprecipitated using Sepharose beads bound to anti-Flag or anti-HA antibodies (Sigma-Aldrich) at 4°C overnight. After washing the Sepharose beads four times with solution B [ 50mM tris-HCl (pH 7.5), 150 mM NaCl, 5 mM EDTA, 0.2% Triton-X100, and 1 mM PMSF], proteins were eluted by heating the beads to 98°C in 1xSDS-polycrylamid gel electrophoresis loading buffer [ 50 mM Tris-HCl (pH 6.8), 2% (V/V) SDS, 6% (V/V) glycerol, and 2% (V/V) β-mercaptoethanol]. The eluted was analyzed by Western blotting with the indicated antibodies.

### Gene knockout by the CRISPR/Cas9 system

To knockout PARP11 and PARP12 in A549 and HEK293T cell lines, two small guide RNAs (SgRNAs) (~100 bp gap sequence) targeting the *PARP11* and *PARP12* genes were designed and cloned into sgRNA expression vectors under the control of human U6 promotor. A549 or HEK293T cells were transfected with sgRNAs and Cas9 expression plasmids, followed by puromycin selection, as described previously (35, 36). Sigle clones were isolated by FACS and confirmed by PCR genotyping and sequencing.

### RNA isolation, reverse transcription, and PCR

Total RNA from cells or viruses was extracted with the PureLink RNA Extraction kit (Thermo Fisher Scientific). Viral RNA copies were measured by qRT-PCR (37) with the One Step PrimeScript RT-PCR kit (Takara). ZIKV primers and TaqMan probes were described previously (38). Primers used to amplify corresponding genes were obtained from PrimerBank (http://pga.mgh.harvard.edu/primerbank/). SYRB Green qPCR mix (TransGen Biotec) was used to analyze mRNA levels on an ABI 7500 (Applied Biosystems) analyzer.

### Immunofluorescence staining and confocal imaging

Vero cells were seeded in a confocal dish (Solarbio) and transfected with EGFP-PARP12 and DsRed-PARP11 plasmids. After 24 hr, cells were fixed with 0.4% paraformaldehyde for 15 min and permeabilized in 0.2% Triton-X100 for 15 min at room temperature. The cells were washed three times with PBS supplemented with 0.05% Tween-20. Nuclei were stained with 4’6-diamidino-2-phenylindole (Thermo Fisher Scientific). Cells were imaged on a LSM700 (Carl Zeiss) confocal microscope, and the images were analyzed with ImageJ software.

### Statistical analysis

All data were analyzed using Prism software (Graphpad). Statistical evaluation was performed by two-way Student’s *t* test. Data are mean±SEM, and *P* values are indicated by *$P$0.05, **$P$0.01, ***$P$0.001 and ****$P$0.0001. All cellular experiments were repeated at least three times.

## Declarations

### Ethics approval and consent to participate

Not applicable.

### Consent for publication

Written informed consent for publication was obtained from all participants.

### Availability of data and materials

The datasets used or analyzed during the current study are available from the corresponding author on reasonable request.

### Competing Interests

The authors have declared that no conflict of interest exists.

### Funding

This project is supported by the CAMS Initiative for Innovative Medicine (No. 2016-I2M-1-005, 2019-I2M-1-003), National Natural Science Foundation of China (91542201, 81590765, 82073181, 81802870), US

National Institute of Health funds (AI069120, AI056154, AI078389 and AI028697), the UCLA AIDS Institute and UCLA David Geffen School of Medicine–Eli and Edythe Broad Center of Regenerative Medicine and Stem Cell Research Award Program, Natural Science Foundation of Jiangsu Province Grant (BK20170407, BK20151253) and Non-profit Central Research Institute Fund of Chinese Academy of Medical Sciences (3332018131, 2020-PT310-006). LL is supported by Chinese Postdoctoral Science Foundation (2019M650564) and Innovative and Entrepreneurial Doctor grant (2020-2022) from Jiangsu Province.

### Authors' contributions

G.C. H.Y. and L.L. jointly designed this study. L.L., S.Z., N.S., and J.L. performed plaque assay and qRT-PCR experiments. L.L., X.X., and L.P. performed Western blotting, coimmunoprecipitation and confocal assay. Y.S., C.P. and L.L. performed CRISPR/Cas9 knocked out assay. G.C., H.Y., S.L. and L.L. wrote and revised the manuscript.

### Acknowledgements

Not applicable.

### Authors' information

Lili Li is an associate professor at the Center for Systems Medicine, Institute of Basic Medical Sciences, Chinese Academy of Medical Sciences & Peking Union Medical College. She has a Ph.D. in cell biology from Chinese Academy of Sciences, and her research interests are anti-viral Interferon-stimulated genes and anti-viral innate immunity.

## References

1. Dick GW, Kitchen SF, Haddow AJ. Zika virus. I. Isolations and serological specificity. Trans R Soc Trop Med Hyg. 1952;46(5):509–20.
2. Singh RK, et al. Zika virus - emergence, evolution, pathology, diagnosis, and control: current global scenario and future perspectives - a comprehensive review. Vet Q. 2016;29:1–26.
3. Sharma V, et al. Zika virus: an emerging challenge to public health worldwide. Can J Microbiol. 2020;66(2):87–98.
4. Kazmi SS, Ali W, Bibi N, Nouroz F. A review on Zika virus outbreak, epidemiology, transmission and infection dynamics. J Biol Res (Thessalon). 2020;27:5.
5. Bhardwaj S, Gokhale MD, Mourya DT. Zika virus: Current concerns in India. Indian J Med Res. 2017;146(5):572–5.
6. Kasprzykowski JI, et al. A recursive sub-typing screening surveillance system detects the appearance of the ZIKV African lineage in Brazil: Is there a risk of a new epidemic? Int J Infect Dis. 2020;96:579–81.

7. Lupia T, et al. 2019 novel coronavirus (2019-nCoV) outbreak: A new challenge. J Glob Antimicrob Resist. 2020;21:22 – 7.
8. Muller WJ, Mulkey SB. Lessons about early neurodevelopment in children exposed to ZIKV in utero. Nat Med. 2019;25(8):1192–3.
9. Luo M, et al. IL-6 and CD8 + T cell counts combined are an early predictor of in-hospital mortality of patients with COVID-19. JCI insight. 2020;9;5(13).
10. Wang J, et al. Cytokine storm and leukocyte changes in mild versus severe SARS-CoV-2 infection: Review of 3939 COVID-19 patients in China and emerging pathogenesis and therapy concepts. J Leukoc Biol. 2020;108(1):17–41.
11. Rasmussen SA, Jamieson DJ. Teratogen update: Zika virus and pregnancy. Birth Defects Res. 2020;112(15):1139–49.
12. Lipworth B, et al. Weathering the Cytokine Storm in Susceptible Patients with Severe SARS-CoV-2 Infection. J Allergy Clin Immunol Pract. 2020;8(6):1798–801.
13. Chakraborty C, et al. SARS-CoV-2 causing pneumonia-associated respiratory disorder (COVID-19): diagnostic and proposed therapeutic options. Eur Rev Med Pharmacol Sci. 2020;24(7):4016–26.
14. Bernatchez JA, et al. Drugs for the Treatment of Zika Virus Infection. J Med Chem. 2020;63(2):470–89.
15. Xie X, Shan C, Shi PY. Restriction of Zika Virus by Host Innate Immunity. Cell Host Microbe. 2016;19(5):566–7.
16. Zhu X, et al. IFITM3-containing exosome as a novel mediator for anti-viral response in dengue virus infection. Cell Microbiol. 2015;17(1):105–18.
17. Snyder B, et al. Synergistic antiviral activity of Sofosbuvir and type-I interferons (alpha and beta) against Zika virus. J Med Virol. 2018;90(1):8–12.
18. Li L, et al. PARP12 suppresses Zika virus infection through PARP-dependent degradation of NS1 and NS3 viral proteins. Sci Signal. 2018;11:535.
19. Li C, et al. 25-Hydroxycholesterol Protects Host against Zika Virus Infection and Its Associated Microcephaly in a Mouse Model. Immunity. 2017;46(3):446–56.
20. Bock FJ, Chang P. New directions in poly(ADP-ribose) polymerase biology. FEBS J. 2016;283(22):4017–31.
21. Aravind L, et al. The natural history of ADP-ribosyltransferases and the ADP-ribosylation system. Curr Top Microbiol Immunol. 2015;384:3–32.
22. Rack JGM, Palazzo L, Ahel I. (ADP-ribosyl)hydrolases: structure, function, and biology. Genes Dev. 2020;34(5–6):263–84.
23. Kuny CV, Sullivan CS. Virus-Host Interactions and the ARTD/PARP Family of Enzymes. PLoS Pathog. 2016;12(3):e1005453.
24. Daugherty MD, et al. Rapid evolution of PARP genes suggests a broad role for ADP-ribosylation in host-virus conflicts. PLoS Genet. 2014;10(5):e1004403.

25. Fehr AR, et al. The impact of PARPs and ADP-ribosylation on inflammation and host-pathogen interactions. Genes Dev. 2020;34(5–6):341–59.
26. Grigg C, et al. Talimogene laherparepvec (T-Vec) for the treatment of melanoma and other cancers. Semin Oncol. 2016;43(6):638–46.
27. Aravind L. The WWE domain: a common interaction module in protein ubiquitination and ADP ribosylation. Trends Biochem Sci. 2001;26(5):273–5.
28. Gibson BA, Kraus WL. New insights into the molecular and cellular functions of poly(ADP-ribose) and PARPs. Nat Rev Mol Cell Biol. 2012;13(7):411–24.
29. He F, et al. Structural insight into the interaction of ADP-ribose with the PARP WWE domains. FEBS Lett. 2012;586(21):3858–64.
30. Guo X, et al. The zinc-finger antiviral protein recruits the RNA processing exosome to degrade the target mRNA. Proc Natl Acad Sci USA. 2007;104(1):151–6.
31. Meyer-Ficca ML, et al. Spermatid head elongation with normal nuclear shaping requires ADP-ribosyltransferase PARP11 (ARTD11) in mice. Biol Reprod. 2015;92(3):80.
32. Saha D, Wakimoto H, Rabkin SD. Oncolytic herpes simplex virus interactions with the host immune system. Curr Opin Virol. 2016;21:26–34.
33. Zhang FC, et al. Excretion of infectious Zika virus in urine. Lancet Infect Dis. 2016;16(6):641–2.
34. Liu SY, et al. Interferon-inducible cholesterol-25-hydroxylase broadly inhibits viral entry by production of 25-hydroxycholesterol. Immunity. 2013;38(1):92–105.
35. Cong L, et al. Multiplex genome engineering using CRISPR/Cas systems. Science. 2013;339(6121):819–23.
36. Mali P, et al. RNA-guided human genome engineering via Cas9. Science. 2013;339(6121):823–6.
37. Johnson BW, Russell BJ, Lanciotti RS. Serotype-specific detection of dengue viruses in a fourplex real-time reverse transcriptase PCR assay. J Clin Microbiol. 2005;43(10):4977–83.
38. Deng YQ, et al. Isolation, identification and genomic characterization of the Asian lineage Zika virus imported to China. Sci China Life Sci. 2016;59(4):428–30.

# Figures

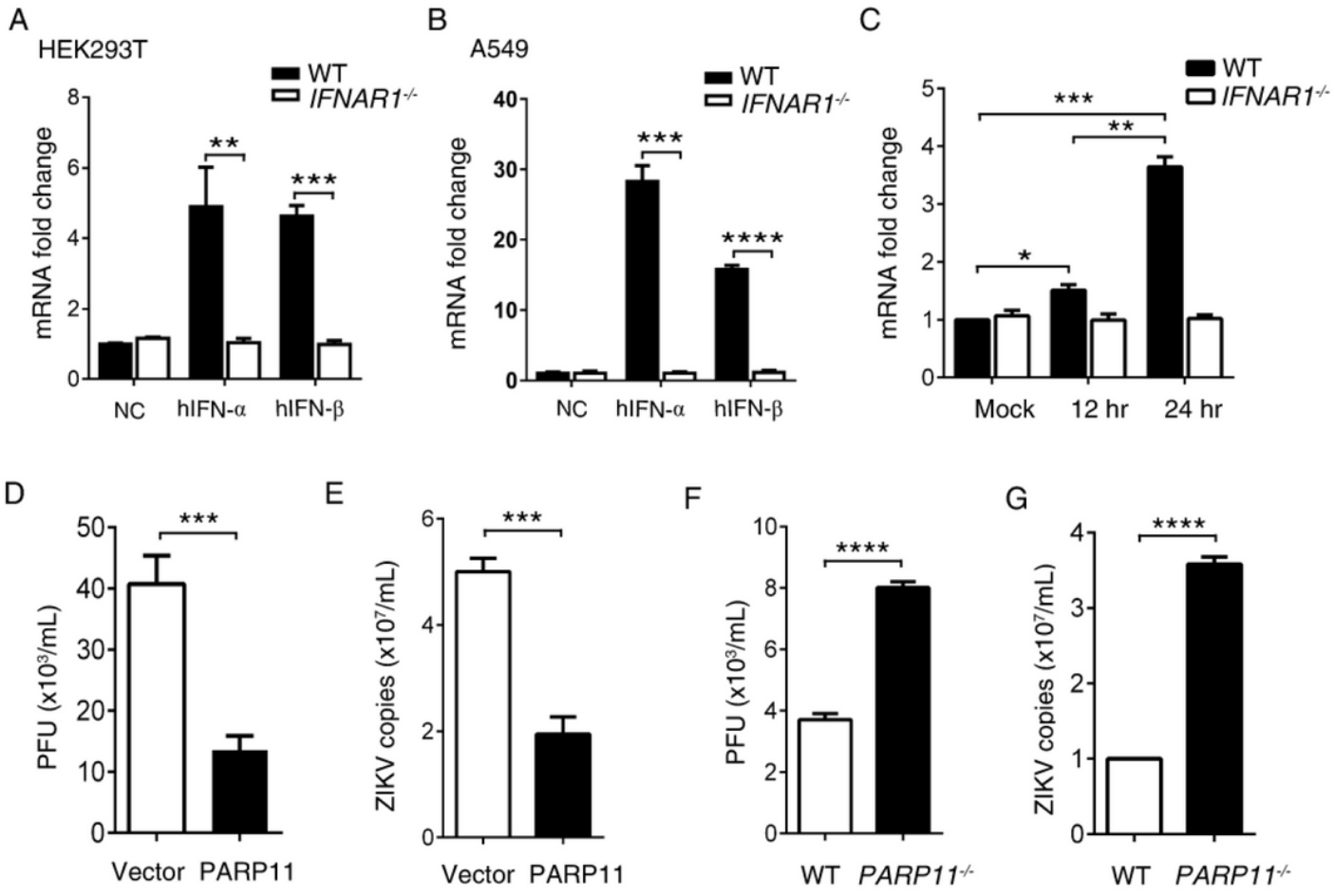


## Figure 1

Type I IFN induced PARP11 suppresses ZIKV replication. (A, B) qRT-PCR analysis of PARP11 expression in wild type (WT) and IFNAR1-/- HEK293T (A) or A549 (B) cells were treated with recombinant human IFN-α (1000 U/mL), IFN-β (20 ng/mL) and control for 24 hr. (C) qRT-PCR analysis of PARP11 expression in wild type (WT) and IFNAR1-/- A549 cells infected with ZIKV for the indicated times. (D, E) PARP11-overexpressing or control vector-transfected A549 cells were infected with ZIKV. Viral accumulation after 24 hr in the culture supernatants (D) and cell lysates (E) were measured by plaque assay (D) or qRT-PCR (E). PFU, plaque-forming unites. (F, G) PARP11-/- or WT A549 cells were infected with ZIKV. Viral accumulation after 24 hr in the culture supernatants (F) and cell lysates (G) were measured by plaque assay (F) or qRT-PCR (G). qRT-PCR and viral titers data (A-G) are mean ± SEM from three independent experiments. *P□0.05, **P□0.01, ***P□0.001 and ****P□0.0001 by Student's t test.

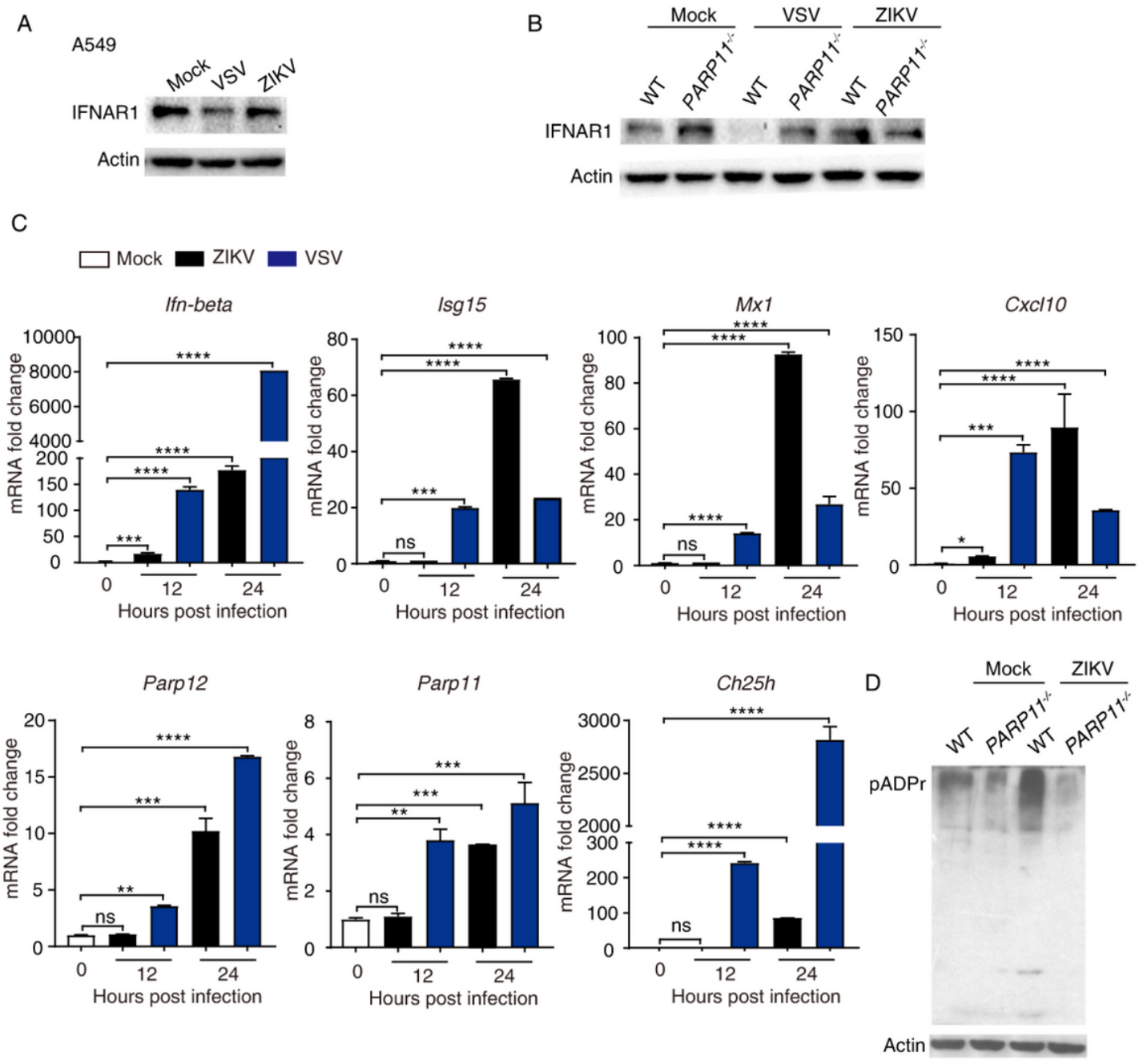


## Figure 2

PARP11 suppresses ZIKV independent on the regulation of IFNAR1 protein level. (A) Western blotting analysis of lysates from A549 cells infected with VSV, ZIKV and mock control. (B) Western blotting analysis of lysates from WT and PARP11-/- A549 cells infected with VSV, ZIKV and mock control. (C) qRT-PCR analysis of ISGs expression in A549 cells infected with ZIKV or VSV for 24 hr and mock control group. (D) Western blotting analysis of lysates from WT and PARP11-/- A549 cells infected with ZIKV and mock control. qRT-PCR data (C) are mean ± SEM from three independent experiments. **P 0.01, ***P 0.001 and ****P 0.0001 by Student's t test. Western blotting results (A, B and D) were presentative of three independent experiments.

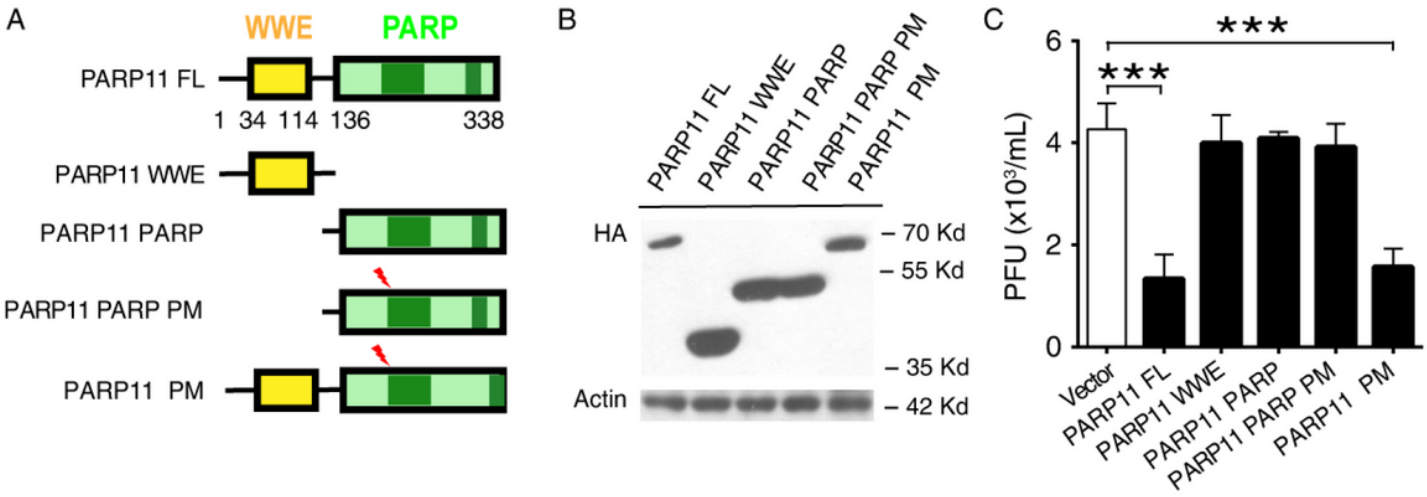


## Figure 3

PARP11 suppresses ZIKV independent on its PARP enzyme activity. (A) Sketch map of the functional regions of full length (FL) PARP11 and mutant constructs. (B) Western blotting analysis of lysates from HEK293T cells transfected with the plasmids encoding recombinant hemagglutinin (HA)-tagged FL and mutant PARP11 constructs. (C) A549 cells were transfected with FL PARP11 and mutant constructs and infected with ZIKV 24hr after transfection. 24hr post infection, ZIKV titers in A549 cells culture supernatant were measured by plaque assay. Western blotting results (B) were presentative of three independent experiments. Viral titers (C) were mean ± SEM from three independent experiments. ***P 0.001 by Student's t test.

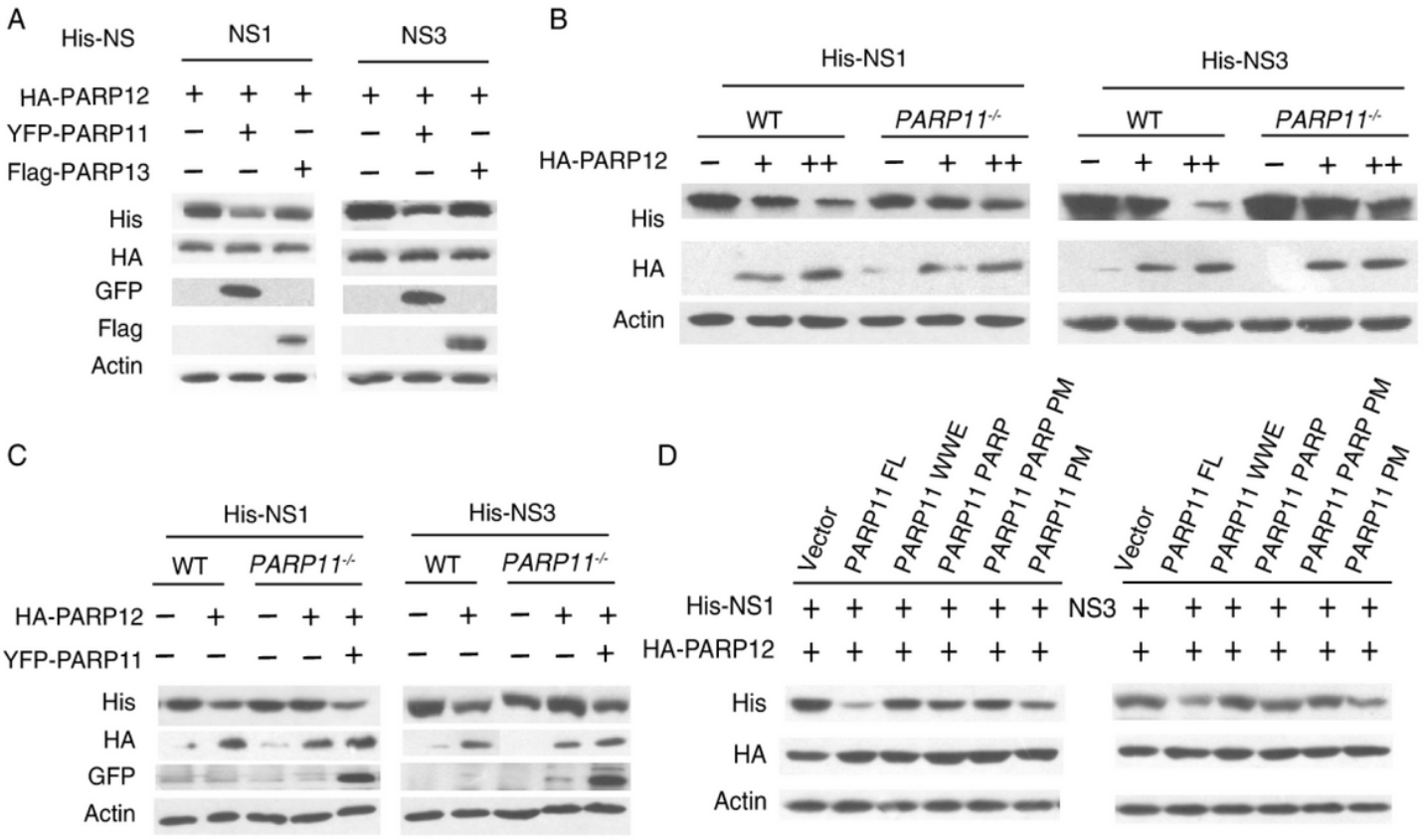


## Figure 4

PARP11 promotes ZIKV NS1 and NS3 protein degradation mediated by PARP12. (A) Western blotting analysis of cell lysates from HEK293T transfected with HA-PARP12, YFP-PARP11, Flag-PARP13 and His-NS1 or His-NS3 plasmids, as indicated. (B) Western blotting analysis of cell lysates from WT and PARP11-/- HEK293T transfected with His-NS1 or NS3 and increasing amounts of HA-PARP12 plasmids (0, 250, 500 ng). (C) Western blotting analysis of cell lysates from WT and PARP11-/- HEK293T transfected with HA-PARP12, YFP-PARP11 and His-NS1 or His-NS3 plasmids. (D) Western blotting analysis of cell lysates from PARP11-/- HEK293T transfected with HA-PARP12, His-NS1/NS3 and FL PARP11 and mutant constructs plasmids. Western blotting results (A-D) were representative of three independent experiments.

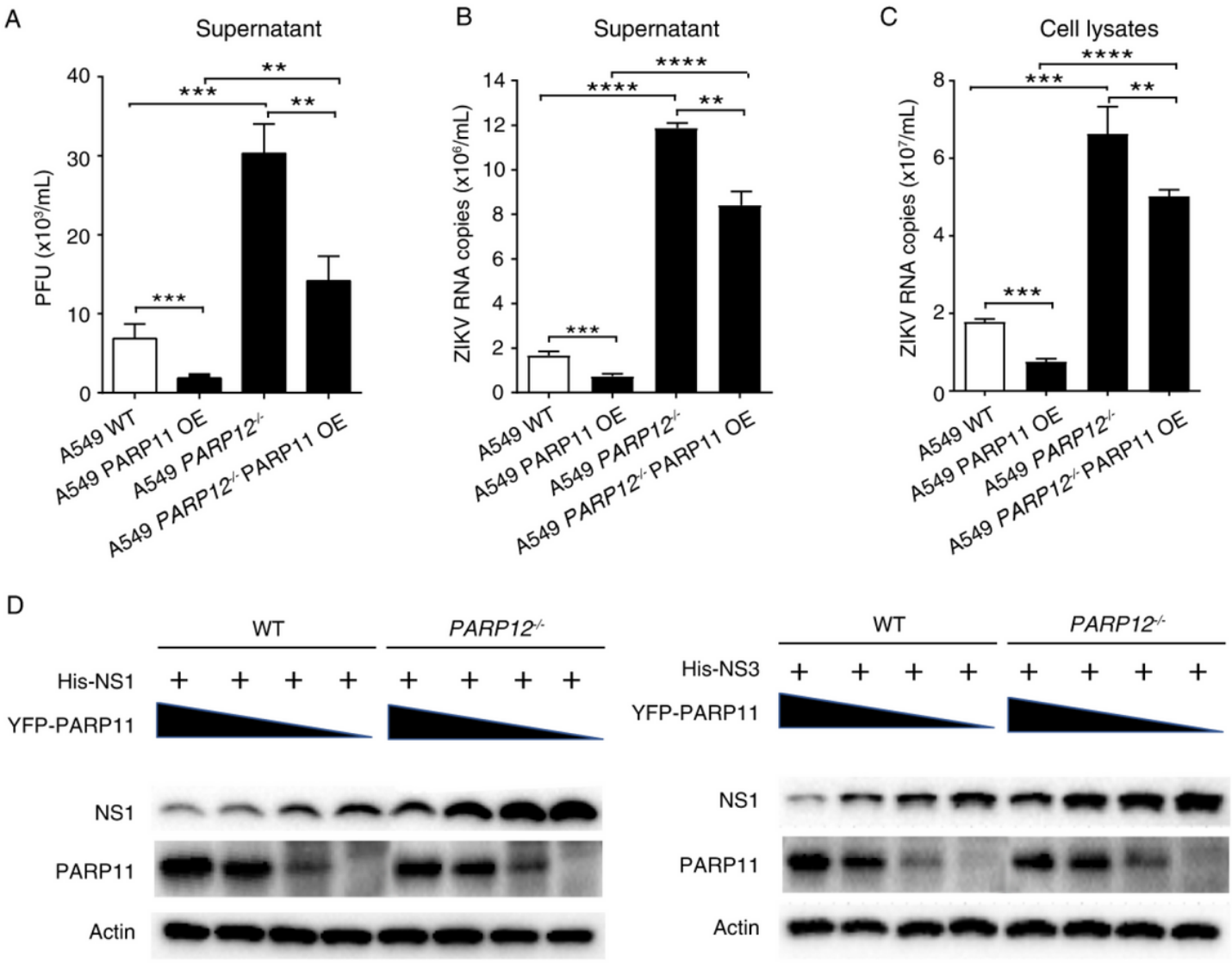


## Figure 5

PARP11 suppresses ZIKV mostly dependent on PARP12. (A-C) PARP11-overexpressing or control vector-transfected WT and PARP12-/- A549 cells were infected with ZIKV. Viral accumulation after 24 hr in the culture supernatants (A and B) and cell lysates (C) were measured by plaque assay (A) or qRT-PCR (B and C). PFU, plaque-forming unites. (D) Western blotting analysis of cell lysates of cell lysates from WT and PARP12-/- HEK293T cells transfected with His-NS1 or NS3 and decreasing amounts of YFP-PARP11 plasmids (500, 300, 100, 0 ng). qRT-PCR and viral titers data (A-C) are mean ± SEM from three independent experiments. **P□0.01, ***P□0.001 and ****P□0.0001 by Student's t test. Western blotting (D) were presentative of three independent experiments.

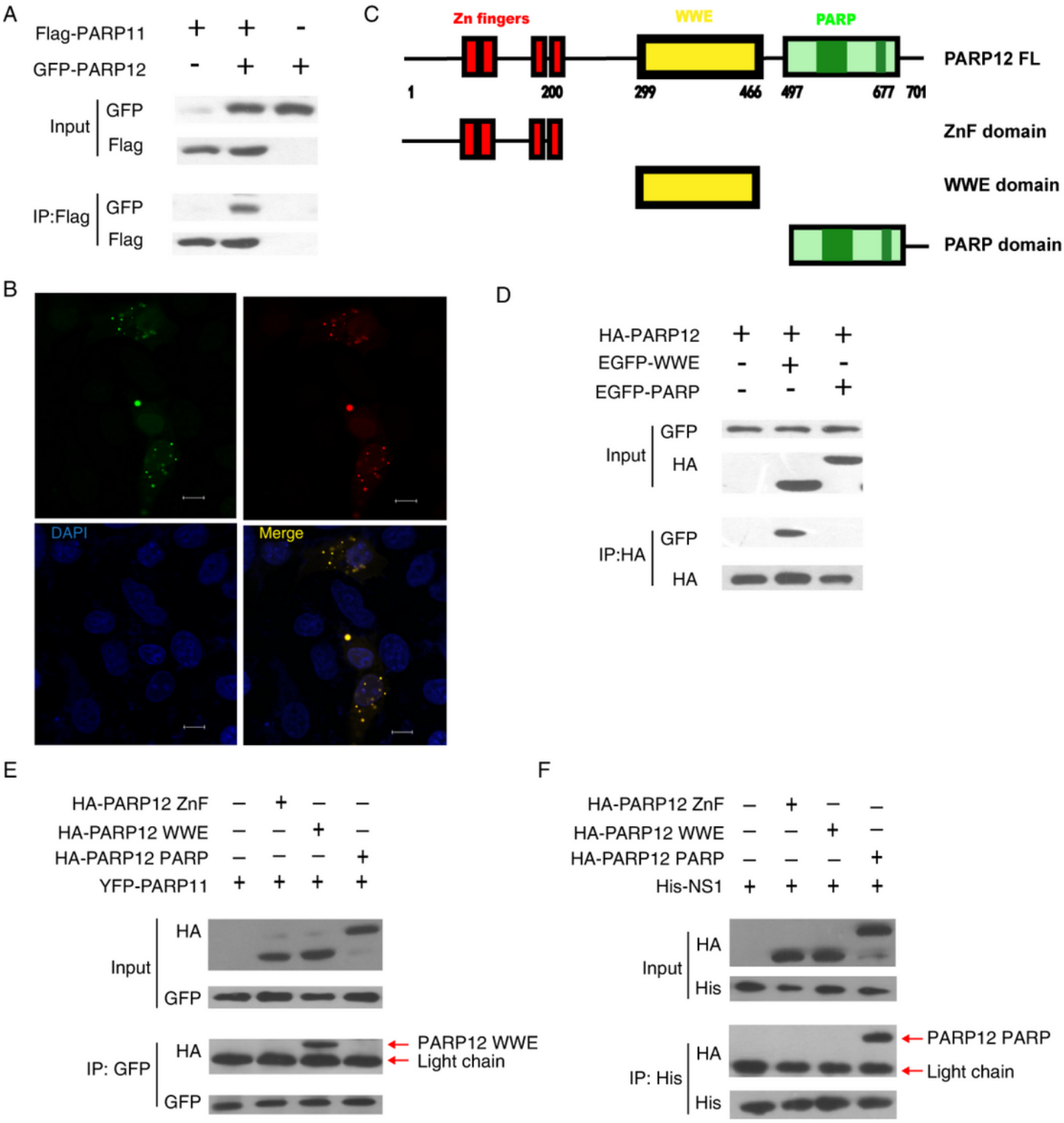


## Figure 6

PARP11 interacts and co-localizes with PARP12. (A) Western blotting analysis of lysates immunoprecipitated for PARP12 from HEK293T cells co-transfected with Flag-PARP11 and GFP-PARP12 plasmids. (B) Confocal microscopy analysis of Vero cells that were co-transfected with EGFP-PARP12 and RFP-PARP11palsmids. Scale bars, 5 μM. (C) Western blotting analysis of lysates immunoprecipitated for PARP12 from HEK293T cells co-transfected with HA-PARP12 and EGFP-WWE or EGFP-PARP

plasmids. Western blotting (A and C) and confocal images (B) were presentative of three independent experiments.

## Supplementary Files

This is a list of supplementary files associated with this preprint. Click to download.

- Supplementarymaterials.docx